

A deep learning approach to concrete water-cement ratio prediction

Sururah Apinke Bello^{a,*}, Lukumon Oyedele^a, Olakunle Kazeem Olaitan^b,
Kolawole Adisa Olonade^c, Akinropo Musiliu Olajumoke^d, Anuoluwapo Ajayi^a,
Lukman Akanbi^a, Olugbenga Akinade^f, Mistura Laide Sanni^b, Abdul-Lateef Bello^e

^a Big Data, Enterprise and Artificial Intelligence Laboratory (Big-DEAL), Bristol Business School University of the West of England, Bristol, United Kingdom

^b Department of Computer Science and Engineering, Obafemi Awolowo University, Ile-Ife, Nigeria

^c Department of Civil Engineering, University of Lagos, Akoka, Nigeria

^d Department of Civil Engineering, Obafemi Awolowo University, Ile-Ife, Nigeria

^e Faculty of Environment and Technology, University of the West of England, Bristol, United Kingdom

^f Department of Computing and Games, School of Computing, Engineering and Digital Technologies, Teeside University, Middlesbrough, United Kingdom

ABSTRACT

Concrete is a versatile construction material, but the water content can greatly influence its quality. However, using the trials and error method to determine the optimum water for the concrete mix results in poor quality concrete structures, which often end up in landfills as construction wastes, thus threatening environmental safety. This paper develops deep neural networks to predict the required water for a normal concrete mix. Standard data samples obtained from certified/leading laboratories were fed into a deep learning model (multilayers feedforward neural network) to automate the calibration of mixing power of the concrete water content for improved water control accuracy. We randomly split the data into 70%, 15% and 15%, respectively, to train, validate and test the model. The developed DNN model was subjected to relevant statistical metrics and benchmarked against the random forest, gradient boosting machines, and support vector machines. The performance indices obtained by the DNN model have the highest reliability compared to other models for concrete water prediction.

1. Introduction

Globally, billions of metric tons of concrete are produced and consumed yearly for construction. This value will continue to rise due to increased development in global economic activities. When adequately proportioned to achieve the desired strength, concrete is the vital construction material for sustainable infrastructural development, and water is the critical input to the concrete hydration for strength and durability properties [1]. However, failure to achieve the assumed compressive strength at design stages may have adverse effects on the anticipated performance of the reinforced concrete (RC) structural elements. Furthermore, research has established that concrete quality and durability is greatly influenced by the quantity of mixing water ([1,2], and most times, this water content is determined based on trial or experience, which may not achieve the required compressive strength. In some regions, the use of low-quality concrete and mismatching production of the concrete mix due to trial-error of mixing has triggered the rising number of material misuse and waste. These give rise to Recycled Concrete (RC) as a result of wastes from building collapse and

demolition [3–5]. The consequences of this include threatened environmental safety due to construction wastes ending up in landfills, increased project costs resulting from building collapse, destruction of civil engineering infrastructures, and loss of human lives.

Aggregates account for about 70–80% of concrete, and their varied chemical compositions (due to climatic conditions) influence the concrete properties, either in fresh or hardened states [6]. Analysis of experimental data by Liu in 1997 [7] has shown that the strength of concrete does not depend on the quantity of cement paste alone but on the effect of the quantity of water required to mix the concrete to a workable level. This property emphasizes the significant impact the mixing water has on the strength and durability of concrete. The quality and performance of concrete both in fresh and hardened states are closely related to the quantity of water used [8–10]. The generally accepted Abrams generalization law in civil engineering [11], expressed as $f = \frac{A}{Bw/c}$, where f is compressive strength, w/c is the water to cement ratio by volume, shows an inverse relationship between the compressive strength and quantity of mixing water (w/c) of concrete mix. Thus, increasing the w/c beyond the optimum value decreases the concrete compressive strength, whereas reducing the w/c ratio down to the

* Corresponding author.

E-mail addresses: Sururah.Bello@uwe.ac.uk (S.A. Bello), L.Oyedele@uwe.ac.uk (L. Oyedele), olaitandoublekay@gmail.com (O.K. Olaitan), kolonade@unilag.edu.ng (K.A. Olonade), aolajumo@oauife.edu.ng (A.M. Olajumoke), Anuoluwapo.Ajayi@uwe.ac.uk (A. Ajayi), Lukman.Akanbi@uwe.ac.uk (L. Akanbi), Olugbenga.Akinade@uwe.ac.uk (O. Akinade), msanni@oauife.edu.ng (M.L. Sanni), Abdul2.bello@live.uwe.ac.uk (A.-L. Bello).

<https://doi.org/10.1016/j.rinma.2022.100300>

Received 11 April 2022; Received in revised form 10 June 2022; Accepted 3 July 2022

Available online 8 July 2022

2590-048X/© 2022 The Authors. Published by Elsevier B.V. This is an open access article under the CC BY license (<http://creativecommons.org/licenses/by/4.0/>).

Nomenclature	
ANFIS	Adaptive Network-based Fuzzy Inference System
ANN	Artificial Neural Network
CNN	Convolutional Neural Networks
CS	Compressive Strength
DNN	Deep Neural Network
ELM	Extreme Learning Machine
FIS	Fuzzy Inference System
FL	Fuzzy Logic
FPNN	Fuzzy Polynomial Neural Networks
FRP	Fiber Reinforced Polymer
GA-ANN	genetic-Algorithm Artificial Neural Network
GBM	Gradient Boosting Machines
HPC	High Performance Concrete
LWC	Light Weight Concrete
MAE	Mean Absolute Error
ML	Machine Learning
MLR	Multiple Regression Analysis
MRA	Multiple Regression Analysis
NA	Natural concrete
OT	Operation Tree
R ²	Coefficient of Correlation
RAC	Recycled Aggregate Concrete
RC	Recycled Concrete
RCPT	Rapid Chloride Penetration Test
RF	Random Forest
RMSE	Root Mean Square Error
RT	Regression Tree
SFLSIM	Self-adaptive Fuzzy Least squares Support vector machines Inference Model
SVM	Support Vector Machines
SVR	Support Vector Regression
UPV	Ultrasonic Pulse Velocity
w/c	Water-cement ratio

optimum value boosts the concrete strength. However, this rule assumed no air void, and the procedure for determining variables A and B is complicated. Also, these two parameters are also influenced by other parameters, i.e., slump, cement type, specimen curing and testing methods, and the age of testing.

In practice, the correct practice to achieve better concrete performance includes using appropriate mix proportioning that considers the multiple impacts of water, followed by effective control of the quantity of mixing water and curing method [12]. The high content of adversely mixing water can influence the properties of fresh concrete by causing an increase in its workability but leading to low strength development [13,14]. Fresh concrete is expected to be workable and easily flowing for ease of placement, compaction, and finishing; these require water beyond the optimum value. In some cases, such excess water beyond the optimum value deliberately injected into the fresh concrete mix to improve its flow and ease of placement could cause segregation and bleeding of the concrete if not adequately controlled. This gives rise to weak concrete and degrades the quality of the final concrete product [15]. Advantages of a properly prepared fresh concrete mix are: (i) prolonged life span of concrete properties and protection from damages resulting from failed or demolished RC structures, and (ii) minimization of environmental impacts from the demolished poor-quality RC.

In optimizing the required water for a fresh concrete mix, techniques such as water-reducing admixtures or superplasticizers have been introduced [6,16], and [17]. However, the use of water-reducing admixtures or plasticizers is an additional cost to the production of concrete which may not be affordable to low-income earners. Popovics [18] emphasized the need for an optimized concrete mixture (i.e., increased workability and improved concrete properties with less water) using reliable and accurate techniques to model concrete materials' behavior. In addition, Machine Learning (ML) models can assist in reducing construction wastes generated through trial mixes of concrete, rejected ready-mix concrete for inadequate flow properties, or demolition of structural elements that failed to meet the minimum strength requirement. For instance, regression analysis has limited ability to model complex nonlinear relationships in concrete mix ingredients and final concrete properties [19], due to many different concrete constituents with properties that can be individually and collectively varied. However, controlling water content concerning the behavior of concrete material is demanding, as water has an enormous influence on the behavior of fresh and hardened concrete. The concrete's strength and durability are dependent on the amount of water, and so are concrete shrinkage and concrete workability [1]. Thus, maintaining the quality of the hardened product for short or long terms and the ability to

consolidate and finish the fresh concrete with uniformity and predictability depends on controlling the water content. However, little or no attention has been devoted to predicting water requirements for conventional concrete mixes. Hence, managing concrete water effectively requires adopting robust methods to predict and manage concrete water content for improved water control accuracy.

Deng et al. [20] argued that deep neural networks (DNNs) are best suited for this problem because of the complex relationships between components in the concrete mix. Thus, to address the issues associated with trial and incorrect mixes of concrete, we adopt this robust technique to manage the require water for concrete mixes to reduce wastage associated with trial mixes and those originating from collapse structures due to incorrect concrete mixtures. Accordingly, the following are the specific objectives of this study:

- 1) construct a deep learning model to effectively model and manage the required water for concrete mixes.
- 2) benchmark the performance of the deep learning model with Random Forest (RF), Gradient Boosting Machines (GBM), and Support Vector Machines (SVM) models.
- 3) interpret the DNN model internal operations using model-agnostic interpretation methods.
- 4) develop a prototype to support informed decision-making to manage the complexity of the concrete material behavior regarding concrete water content.

Consequently, this paper develops a tool to manage the required water quantity for concrete mixes; and compares its performance with selected ML models using the root mean square error, mean absolute error, forecast bias, and coefficient of correlation (R^2). This tool will help stakeholders make informed decisions regarding the managing operations of concrete water content for durable concrete production that guarantees safe structures and reduces construction waste.

The remainder of the paper is structured as follows: In Section 2, a review of literature is carried out. Section 3 discusses the methodology employed in this study to develop predictive models, a form of data analytics using current and historical data to forecast activity, behavior, and trends. Results evaluation is in section 4, while the implication of the study in practice is discussed in Section 5, and Section 6 concludes the paper.

2. Literature review

2.1. Application of computational models in assessing concrete properties

The emergence of new concrete mixtures and applications has motivated the need for accurate predictions of relevant concrete properties (i.e., strength, slump, elasticity). A summary of ML approaches to predetermining concrete properties is shown in Table 1. Essentially, the relationship between concrete components (compressive strength, elastic modulus, tensile strength, permeability, water-cement ratio, density, water absorption and crush index, sand ratio, cement dosage, aggregates ratio, and other factors) is a complex nonlinear relationship. However, modeling techniques, for instance, can derive some analytical mathematical functions using experimental data [21] and system properties defined with pure mathematical models. However, mathematical models cannot provide insights into the workings of systems and

Table 1
Applications of ML techniques and concrete properties.

Author	Approach	Area of Study
[22]	ANN	CS of HPC
[23]	ANN	CS of natural concrete
[24]	BP-ANN	CS of natural concrete
[25]	ANN	Confined CS and Strain of circular concrete columns
[26]	ANN	Fracture parameters of concrete
[27]	ANN	Modulus elasticity of RA
[28]	ANN (CC and BP)	CS of structural light weight concrete
[29]	ANN	Long-term effects of fly ash and silica fume on CS
[30]	ANN	CS, tensile strength, gas permeability and chloride ion penetration of HPC
[31]	ANN	CS of ground granulated blast furnace slag concrete
[32]	ANN	Permeability of chloride ions on a varied mix of HPC
[33]	ANN	CS of RAC with varied aggregates
[34]	BP-ANN	Slump, CS and elastic modulus of RAC
[35]	ANN	Model the velocity–strength relationship of concrete
[36]	ANN	CS using UPV and density values for reinforced concrete structures
[37]	ANN and MRA	CS of concrete
[38]	ANN and FL	Compressive strength of silica fume concrete
[39]	Second-order regressions and ANN	Slump flow of concrete
[40]	MRA and ANN	CS of concrete containing blast furnace slag and fl ash
[41]	ANN and fuzzy logic	CS of concretes containing fly ashes
[42]	Fuzzy NN and FPNN	CS of natural concrete
[43]	ANN, FIS and ANFIS	CS of HPC
[44]	Hybridized OT and GA	CS of HPC
[45]	Regression, ANN and ANFIS	CS of no-slump concrete
[46]	SVR	CS and RCPT of concretes containing metakaolin
[47]	Geometric Semantic GA	CS of HPC
[48]	Ensemble Decision Tree	CS for HPC
[49]	ANFIS and GA-ANNs	CS of concrete
[50]	M5' Algorithm	Modulus elasticity of RAC
[51]	Self-adaptive FIS based SVM	Compressive strength of rubberized concrete
[52]	Multivariable regression and GA	Modulus of elasticity and the splitting tensile strength of structural recycled concrete
[53]	ANN and regression	Relationships between RAC components and properties
[54]	SVM	CS of FRP confined concrete
[20]	CNN	CS of RAC
[55]	ELM	CS of lightweight foamed concrete
[56]	ANN-GA	Slump of ready-mix concrete
[57]	RF and SVM	Modulus of elasticity of RAC
[58]	RT, RF and GBM	CS and splitting tensile strength

essential dependencies between variables.

Thus, they perform poorly in dealing with complex and uncertain environments, such as predicting material properties in concrete mix designs [59]. Accordingly, empirical and statistical models, such as linear regression, have been used to model concrete properties [39,52]. However, regression models require laborious experimental work to develop and may produce inaccurate results when the relationships between concrete properties are complex. Due to their important characteristics, i.e., the ability to learn from data and fault tolerances, artificial neural networks (ANNs) have been used as alternative approaches to model concrete properties [27,31,34,36,50,53]. For instance, in predicting CS, Bilim et al. [31] collected 225 data samples to develop a feedforward, single hidden layer neural network and obtained a high-performance R^2 of 0.965. Ozcan et al. [38] also adopted a feed-forward network to predict CS using 240 data samples and reported a Squared-R of 0.977. Similarly, Duan [33] used 168 sets of experimental data to develop a back-propagation network model, which produced R^2 and RMSE values of 0.996 and 3.680, respectively, on the testing set. Zarandi et al. [42] developed fuzzy polynomial neural networks for CS prediction using 458 experimental data of different concrete mix designs, and $R^2 = 0.8209$ was obtained as the best prediction ability. Shao et al. [34] used BP neural networks to model concrete slump and obtained a prediction accuracy of 0.857. Similarly, Yeh [39] used experimental data of 78 records and adopted neural networks and second-order regression for concrete slump flow modeling. The performance ability of ANN concerning R^2 was 0.72 on the testing set.

However, ANNs still suffer from uncontrolled convergence speed, poorer generalization performance, and overfitting problems. Also, parameters of neural networks greater than two layers are difficult to optimize using the traditional gradient descent. Furthermore, SVMs and SVRs have low computational costs, accessible optima, and are efficient for small data sample problems. Consequently, they have been applied to model concrete properties [46,51,54]. For example, Mozumder et al. [54] used SVR on 238 samples to predict the uniaxial compressive strength of FRP confined concrete and obtained performance metrics $R^2 = 0.9832$ and RMSE = 8.59 on the testing data. Nevertheless, the computational complexity of SVMs grows exponentially with the training sample size. Decision trees [50,58] have also been used as a non-parametric tool based on induction rules to analyze the concrete mix data. However, they have poor generalization ability, especially for examples not in the training set. Recently, ML techniques, i.e., random forests [57,58] gradient boosting machines [58], have made great attempts at modeling concrete mix data to predict concrete properties. However, error rates are still unsatisfactory.

However, the major challenge associated with most conventional ML and statistical techniques is the considerable effort to manually extract data attributes to achieve good prediction performance. In addition to this challenge are the nonlinear relationships with high-order interactions among variables. Consequently, due to their good generalization ability and robust mechanisms for handling sparse, noisy, and nonlinear data, deep learning techniques are being proposed to address these challenges. Data and algorithm-level methods are continuously improving, and current research activities are focusing on computationally efficient data analysis methods. Moreover, unsupervised and supervised learning techniques are combined in deep learning to yield a semi-supervised model, an attribute lacking in the conventional ML techniques. Thus, deep learning has motivated successful applications, i.e., face recognition [60], sound analysis [61], defect detection [62], fault diagnosis [63], safety analytics [64], and demolition waste analysis [65]. Additionally, deep learning techniques have outperformed methods like principal component regression, support vector machines, and shallow artificial neural networks due to their remarkable representation ability [66].

Similarly, based on the reviewed past studies on modeling concrete properties, it can be concluded that the experimental samples are small. Also, most of the studies emphasized more on determining the

compressive strength of the concrete with little effort to managing the water required for concrete mix. The reason attributed to this fact is that improving the compressive strength of concrete will automatically enhance its other properties (density, shear strength, modulus of elasticity, permeability). However, it should be noted that the concrete's strength and durability are dependent on the amount of water in the fresh mixture (and subsequently the pore space in the hardened mass). The concrete shrinkage property is also proportional to water content, and workability is exponentially dependent on water. Water thus exerts its influence on the behavior of the fresh and hardened concrete to the degree that is perhaps greater than other variable ingredients of the mixture. Controlling concrete water content due to the complexity of the concrete material behavior is demanding. Also, maintaining the quality of the hardened product for short or long terms and the ability to consolidate and finish the fresh concrete with uniformity and predictability depends on controlling the water content. To the best of our knowledge, deep learning applications for optimal concrete water control have not been profound in concrete mix designs. Thus, managing water effectively requires adopting robust methods that predict concrete water content for improved water control accuracy.

Thus, we chose deep neural networks to manage concrete water content in this study and benchmarked their predictive performance with the popular techniques for modeling concrete properties, i.e., gradient boosting machines (GBM), random forest (RF), and support vector machines (SVM). GBM and RF have been shown to outperform other conventional ML models, i.e., decision trees, in predicting concrete mechanical properties [58], while SVM has low computational costs and accessible optima.

2.2. Justification for the study

The need to efficiently control water contents to maintain the quality of hardened products for short or long terms is highly demanding. More so, traditional ANNs show good prediction abilities; however, their slow convergence, overfits, and local optimization affect the accuracy and efficiency of predictions [36]. Also, the prediction accuracy of the conventional machine learning methods is largely dependent on effective parameters selection. In comparison, deep learning techniques can learn complex relationships and patterns in massive datasets even with missing entries [60] and have achieved great success in face recognition, sound analysis, fault diagnosis defect detection [67]. In predicting concrete properties, though deep learning techniques have been used [20,68–75], due to their generalization ability and mechanisms for handling sparse, noisy, and nonlinear data. However, to the best of our knowledge, limited studies exist that employ deep learning techniques for predicting the required water for concrete mix.

This study adopts deep learning techniques and develop a prototype to estimate the required water for concrete mixtures with no chemical admixtures, which is helpful in environments where superplasticizer is unpopular, especially, in developing countries, because of additional costs. This study is needed to prevent frequent building collapse due to poor-quality concrete, especially in developing countries. Furthermore, effective water management in concrete requires robust and efficient methods capable of modeling complex nonlinear systems, i.e., controlling concrete water content for improved quality water control accuracy.

2.3. Deep neural networks

A deep neural network is a function that maps an input vector to an output vector and has emerged as a highly successful field of machine learning [76,77]. Deep neural networks (DNNs) are the new direction for traditional machine learning technologies, inspired by the mechanism of mammalian brain recognition [62]. Deep neural networks (DNNs) with their multiple nonlinear hidden layers enhance the learning of complicated relationships between their inputs and outputs.

The first layer (input) has neurons activation set to the value of the input vector. The last layer (output layer) represents the output vector, and the intermediate layers (hidden layers) give intermediate representations of the input vector. In contrast to artificial neural networks with only one hidden layer and few hidden neurons per layer, DNNs comprise many hidden layers with a significant number of neurons. The goal is no longer to learn the main pieces of information but to capture all possible facets of the input [78]. Considering a neural network with H numbers of hidden layers, also let $h \in \{1, \dots, H\}$ represents the index of the hidden layers in the network. The feedforward operation of a standard neural network can be described as (for $h \in \{1, \dots, H-1\}$ and any hidden unit i , presented in Equations (1) and (2):

$$x_i^{(h+1)} = w_i^{(h+1)}y^h + b_i^{(h+1)} \quad (1)$$

$$y_i^{(h+1)} = f(x_i^{(h+1)}) \quad (2)$$

Where $x^{(h)}$ is the vector of inputs into layer h , $y^{(h)}$ is the vector of outputs from layer h . $w^{(h)}$, $b^{(h)}$ and f denote the weight matrix and biases vector at layer h and the activation function respectively. Basically, the most successful inventions in the context of DNNs are rectified linear units (ReLU) as activation functions [79]. A ReLU function is the identity for positive values and zeroes otherwise. The use of ReLUs gives rise to sparse input representations that are robust against noise and makes classification models more comfortable in higher-dimensional spaces [80]. The most important advantage of ReLU is its remedy for the vanishing gradient, from which networks with sigmoid activation functions and many layers suffer. Also, modern deep neural networks provide training stability, generalization, and scalability with big data [81]. A compressive overview of deep learning methodologies is found in Schmidhuber [77].

3. Methodology

This section discusses the methodology adopted, specifically the dataset and the development of prediction models. The outline is shown in Fig. 1. The concrete considered in the study is ordinary concrete for general construction purposes with no superplasticizer or admixtures. In developing automatic concrete mix designs, we employ multilayer deep feedforward neural networks to predict the required water content for the different concrete mix proportions.

3.1. Theoretical framework

Strength is the most valued property of concrete as it measures its ability to resist stress under loading. The working stress theory for concrete selection prefers compressive strength over tensile and flexural strength because of its comparative advantage to resist compression loading. Although, strength development in concrete is a long-term process due to the relatively slow nature of hydration reaction. In practice, however, concrete strength is usually determined based on controlled curing of concrete tested at selected ages of 3, 7, 14, and 28 days. In a real-life structure, concrete is exposed to multi-directional stress. However, for ease of laboratory test, a uniaxial compression test is universally accepted for testing concrete due to its simplicity [82].

Theoretically, the 28-day strength of concrete is widely accepted as a criterion in selecting concrete strength for design purposes since it is believed to have attained about 99% of its strength at this age of curing under standard temperature-humidity conditions [82]. Meanwhile, 7-day strength is also selected for assessing strength properties and measuring early strength development; and considered for concrete selection where there is a limitation of time for making decisions. In addition, the concrete designer usually predicts 28-day strength from the 7-day strength as it is assumed that the concrete is in the range of 60–75% of 28-day strength [83]. However, seldomly, in practice, the strength of concrete is also measured at 14 days of curing. This

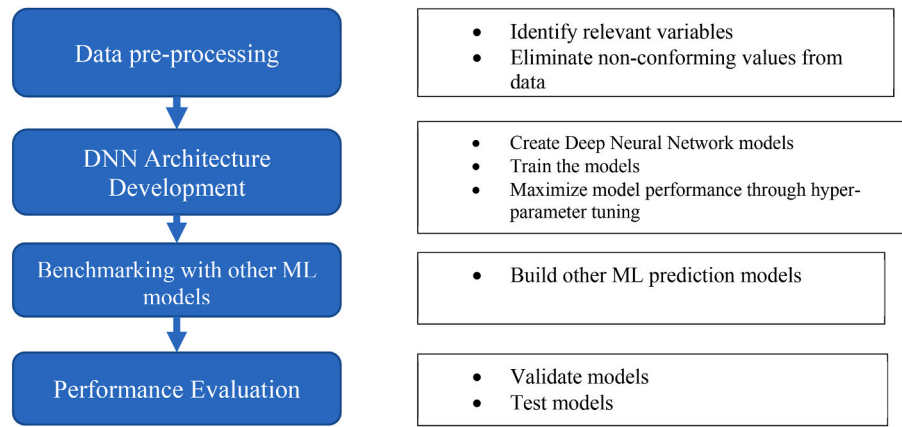


Fig. 1. Flow of the research methodology.

theoretical understanding reflects the concrete mix data collected in this study from different concrete practitioners with 48% based on 28-day strength, 42% on 7-day strength, and 10% measured the strength of concrete at 14 days of curing.

3.2. Data identification and collection

Concrete is a highly complex material, and modeling its behavior is difficult. According to Yeh and Lien [44]; the four basic ingredients of conventional concrete (Portland cement, water, and fine and coarse aggregates) influence its mechanical properties. In this approach, the required water (liter/m^3) for the concrete mix is taken as a function of the following seven input features: cement (kg/m^3), fine aggregates (kg/m^3), coarse aggregates (kg/m^3), concrete compressive strength (N/mm^2), density (kg/m^3), slump (mm), and age of testing (days). The determination of the input vectors was made to ensure that the major parameters influencing the strength of concrete were fairly represented based on the earlier study by Živica [1]. In this study, concrete mixes from ordinary Portland cement were considered to eliminate the effect of cement types on concrete properties. As a result, all factors except the quantity of the concrete component that may affect the properties of mixing concrete as described in Ref. [2] were not considered in our experiment. Portland Cement of grade 42.5R and grade 32.5 N were considered as these are the available grades in Nigeria. Grade 42.5R cement had higher tri-calcium silicate and di-calcium silicate contents than the 32.5 N cement, thus has higher comprehensive strength [84].

A dataset of three thousand and twenty-one (3021) standard concrete tests were collected from ten different standard laboratories. This dataset (certified trial mix) contains the following: date cast, date tested, mix proportion, and cube size (usually $150\text{mm} \times 150\text{mm} \times 150\text{mm}$). Others are cement types (i.e., Ordinary Portland Cement), placing detail, aggregate types, concrete cube density (kg/m^3), crushing load (kN), age (usually 7, 14 and 28 days), water-cement ratio and average compressive strength. Seven components (cement, fine aggregate, coarse aggregate, density, slump, age, and compressive strength) represent the predictor variables, while the attribute water is the output variable. Table 2 shows the quantity of the constituent materials and the water-cement ratio (w/c) of the concrete used in this study, the values of w/c ranged between 0.48 and 0.74. Those with w/c above 0.6 were made with naturally deposited sand as fine aggregate, while those with w/c lesser or equal to 0.60 were made with granite dust as fine aggregate.

This is an indication that the naturally deposited sands contain higher silt fractions (with higher water absorbing tendency) than the granite dust, this would require higher water to achieve adequate workability due to increased surface area. Data pre-processing or normalization eliminates numerical difficulties or conditions where the attributes with greater ranges dominate those with smaller ones. Scaling data input to a range of (0, 1) improves the learning rate drastically [56]. Normalization is carried out by using Eq. (3).

$$X = \frac{(x - x_{min})}{(x_{max} - x_{min})} \quad (3)$$

Table 2

Some details of typical sample of collated concrete data.

Cement (kg/m^3)	Fine Aggregate (kg/m^3)	Coarse Aggregate (kg/m^3)	Age	Concrete Strength (N/mm^2)	Slump	Density (kg/m^3)	Water (liter/m^3)	ratio
289	835.1	1116.7	14	19.64	67	2380	185.0	0.64
277	607.2	1056.3	28	14.78	89	2210	187.7	0.68
286	855.8	1290.1	7	13.88	87	2530	185.0	0.65
348	574.4	981.8	14	29.05	45	2410	186.3	0.53
320	753.6	1048.3	7	15.96	105	2240	184.7	0.58
376	514.8	1239.8	28	30.62	95	2420	185.0	0.49
340	825.8	1126.8	7	22.82	56	2430	218.3	0.64
268	666.3	963.6	28	27.13	79	2520	190.9	0.71
329	845.4	1182.7	14	21.17	98	2300	186.0	0.57
286	801.9	857.6	14	23.96	89	2440	190.3	0.67
388	588.8	1098.7	28	15.19	93	2390	185.3	0.48
350	686.7	1097.5	7	30.62	67	2430	213.1	0.61
326	885.6	995.9	28	9.19	83	2220	184.5	0.57
296	720.4	951.9	7	27.36	67	2220	218.3	0.74
252	614.8	1188.8	28	30.62	101	2230	186.5	0.74
440	718.1	1088.8	7	8.03	79	2120	218.3	0.50
261	767.2	1015	14	26.21	98	2350	182.3	0.70
295	777.9	976.6	7	17.33	100	2130	185.6	0.63
336	717.9	998.2	28	17.64	101	2420	182.2	0.54

Where X is the estimator of the normalized data, x is the sample data collated, x_{\max} is the maximum value and x_{\min} is the minimum value of the data collated. This estimator scales and translates each feature so that all values are in the range 0 and 1, to avoid any of the variable dominating others. This normalization is required since the dataset has input values with different scales; hence, this process accurately estimates the minimum and maximum observable values.

Also, redundant predictors can affect the precision of models and lead to unreliable forecasts. Thus, we used the variance inflation factor (VIF) to measure the degree of collinearity present in the dataset and eliminate redundant predictors. The higher the value of VIF, the higher the collinearity is between the related variables. VIF_j (Eq. (4)) of a predictor x_j is calculated using the linear relationship between x_j and other independent variables $[x_1, x_2, \dots, x_{j-1}, \dots, x_m]$.

$$VIF_j = \frac{1}{1 - R_j^2}, \quad j = 1, \dots, p, \quad (4)$$

where, R_j^2 is the coefficient of determination of the regression of x_j on all other independent variables in the dataset $[x_1, x_2, \dots, x_{j-1}, \dots, x_m]$. In the case when there is no multicollinearity between the variables in the dataset, R_j^2 equals zero, and VIF_j equals 1. However, if multicollinearity exists, VIF_j progresses to a value much greater than 1. James et al. [85] recommended VIF thresholds to detect the multicollinearity phenomenon. VIF values less than five are appropriate, while values greater than five are a cause of concern or indicate serious collinearity. Thus, we included all the seven predictors in the forecasting model development since their VIF values are less than five and satisfy the multicollinearity examining condition.

In addition, data cleaning methods are also employed to detect and repair errors in the data, as described by Chu et al. [86]. For instance, we used the mean substitution technique, the most commonly practiced approach to address missing values by replacing missing values on a variable with the mean value of the observed values. The dataset for model development was split into training (70%), validating (15%), and testing set (15%), respectively. The training data was used to build the models, the validation was used to prevent overfitting, and the test data was used to evaluate the prediction ability of models. Table 3 shows a summary of the variables and their VIF values (except for the dependent variable). Independent variables (features) comprise cement, fine aggregates, coarse aggregates, curing age, slump, density, and compressive strength, while the dependent variable (Q) is the required water (liter/m³).

3.3. DNN topologies and hyperparameter settings

The architecture of the deep learning model shown in Fig. 2 depicts input and output variables for prediction. Usually, creating a simple DNN model starts by using only dense layers as a baseline, then using a smaller model (less hidden units) and then creating a complex model with a capacity in the hidden layer. Finally, the validation losses of these

Table 3

Representation of dependent and independent variables.

Variables	Acronym	Minimum	Maximum	Average	VIF
Coarse Aggregates (x_1) kg/m ³	CA	857.60	1397.50	1095.24	1.10
Cement (x_2) kg/m ³	CEM	213.00	489.00	369.93	2.10
Fine Aggregates (x_3) kg/m ³	FA	514.80	937.60	725.68	1.04
Age (x_4)	AG	7.00	28.00	17.57	4.84
Compressive Strength (x_5) N/mm ²	CS	6.48	30.90	21.76	4.12
Slump (x_6) mm	SLMP	45.00	110.00	83.64	2.19
Density (x_7) kg/m ³	DEN	2000.00	2630.00	2372.98	3.24
Water (Q) liter/m ³	WATER	162.30	218.30	186.53	NA

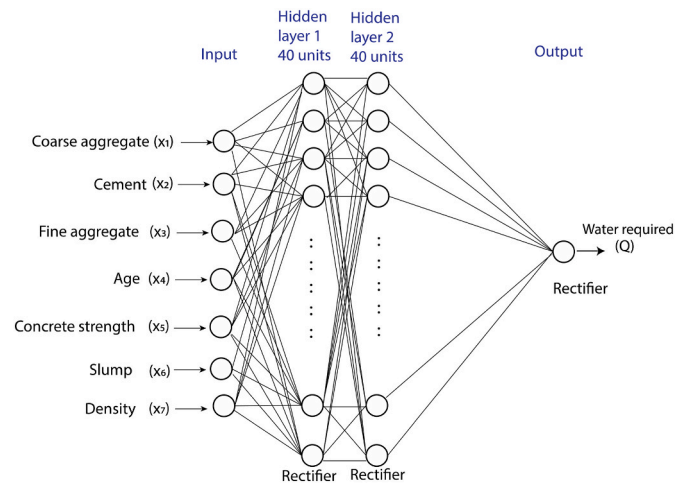


Fig. 2. Deep learning architecture for predicting the required water for concrete mix.

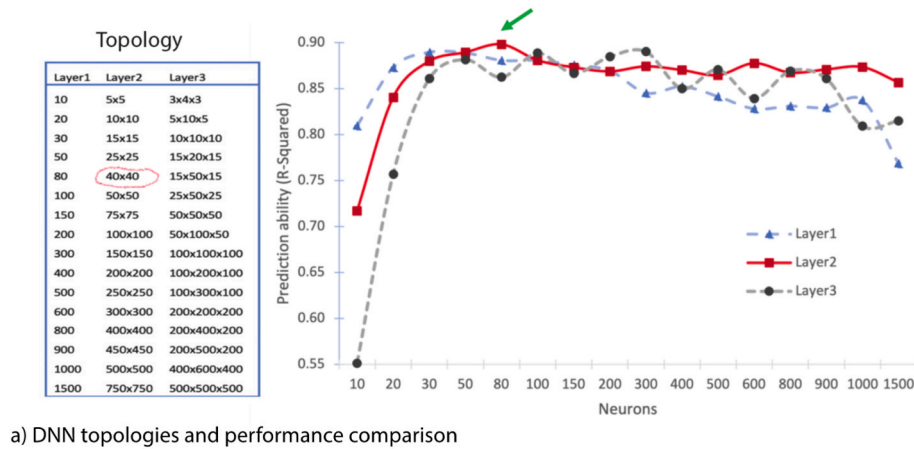
models are compared by benchmarking their performance using appropriate metrics. It should be noted that there is no specific method for determining the right number of layers of the deep learning architecture. However, it is best to start with a few layers and then increase the size until diminishing returns on the validation loss are achieved, as recommended in LeCun et al. [76]. Thus, in determining the number of network layers and neurons, we tried three network topologies, i.e., one layer, two layers, and three layers, using neurons in the range 10–1500 and initially training these networks at 10 epochs to evaluate their predictive abilities on the validation set. The rectifier or Rectified Linear Unit (ReLU) was used as the activation function for the hidden layers and output node. The computed error between the actual and predicted output was propagated backwards. Other neural network hyperparameters are set at default values.

Fig. 3a depicts the network topologies and their performance on the validation set. However, a 2-layer network with 80 neurons (40 neurons in each layer) obtained the highest R-Squared of 0.898; thus, we settled for this topology. However, in arriving at the optimal number of epochs for training the neural networks, we adopted different epoch numbers to study the convergence of the training procedure. Fig. 3b depicts the plot of the mean square error vs. epoch numbers. The model reached convergence at 500 epochs (mean square error = 7.20); hence, we used this value (500) for training the final model. Thus, the overall network architecture comprises an input unit (representing the seven predictors), followed by two rectified layers (hidden units) with 40 neurons each and completed with a final layer output unit. This chosen network topology is less complicated and guarantees model generalization on the test data.

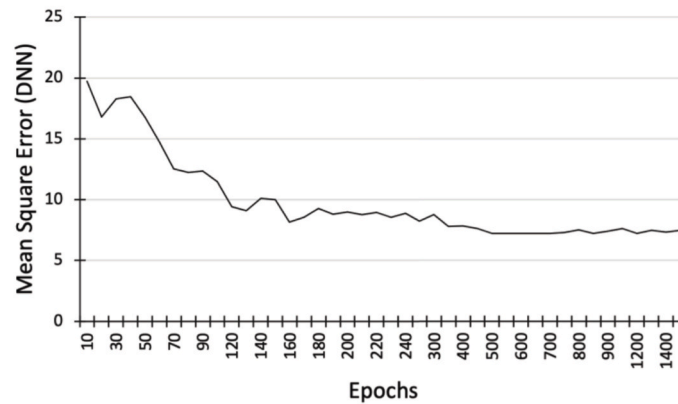
In addressing the overfitting of regularization parameters (Lasso and Ridges) were used as described by Srivastava et al. (2014). For instance, h_1 (H_1 : Lasso) and h_2 (H_2 : Ridge) regularization enforce the same penalties by modifying the loss function to minimize loss as described by Eq. (5):

$$H'(w, b_i) = H(w, b_i) + \lambda_1 R_1(w, b_i) + \lambda_2 R_2(w, b_i) \quad (5)$$

For h_1 regularization, $R_1(w, b_i)$ is the sum of all h_1 norms for the weights and biases in the network; h_2 regularization via $R_2(w, b_i)$ represents the sum of squares of all the weights and biases in the network. w is the collection $\{w_i\}_{1:N-1}$, where w_i denotes the weight matrix connecting layers i and $i+1$ for a network of N layers. Similarly, b is the collection $\{b_k\}_{1:k+1}$, where b_k denotes the column vector of biases for layer $k+1$. The constants λ_1 and λ_2 are generally specified as very small. The gradient descent is a popular algorithm for optimizing neural networks, as it minimizes the objective function $f(\theta)$, $\theta \in \mathbb{R}^d$ by updating parameters in the opposite direction of the gradient of the objective



a) DNN topologies and performance comparison



b) Plot of mean square error vs. epoch numbers

Fig. 3. Experiment with different DNN topologies.

function $\nabla_{\theta} f(\theta)$ w.r.t. to parameters and the learning rate to determine steps taken to reach a (local) minimum. However, the gradient descent can fail to recover the true trajectory due to the cost of gradient computation. Similarly, stochastic gradient descent, which has a robust initialization and annealing schedule, may get stuck in saddle points rather than local minima. Thus, to overcome this challenge, the Nesterov accelerated gradient [87], an efficient optimization technique, was used to reduce the gradient computation cost. The deep learning model was implemented using keras in a Python environment.

3.4. Selected machine learning techniques for benchmarking

To benchmark the performance of the deep learning model, we used three techniques that stand among the most popular and successful supervised Machine Learning (ML) methods namely, Random Forest (RF), Gradient Boosting Machines (GBM), and Support Vector Machines (SVM). Similar approach was found in Refs. [62–64].

3.4.1. Random forest

Random forest algorithm [88] uses decision trees to construct numerous trees by recursive partitioning the predictor space, i.e., using the binary splits to separate regions possessing the closest responses to predictors. For example, in a classification problem, a constant is fit locally on the individual final region to generate the closest probable category to the categorical outcome. However, for regression, the final result is determined using the dependent variable average value. RF derives advantages of trees, which include the ability to express highly complex and nonlinear interactions between predictors, handling outliers, extraneous predictors, and high dimensional data sets of huge observations [58].

Two parameters are often essential when tuning the RF model. These are the number of trees required (*ntree*), and the number of random variables for each tree (*mtry*). Finding the optimal *ntree*, involves setting the *mtry* to the default value (sqrt of total predictors) and then searching the required number of trees from a list, i.e., (40, 60, 80, 120, 160, 200, 240, 280, 320, 360, 400) corresponding to a stable model. We build 10 RF models repeatedly, and for each *ntree*, we note the following: Out of Bag (OOB) error rate and trees with stabilizing OOB error rate reaching the minimum. Similarly, we determine the optimal *mtry*, by applying the same procedure as above; that is, running the RF model ten times, and selecting the optimal number of predictors (i.e., 1, 2, 3, 4, 5) for the split where the out of bag error rate stabilizes and reaches the minimum. The optimal values for these parameters are depicted in Table 4.

3.4.2. Gradient boosting machines

According to Friedman [89], the learning procedure in gradient boosting machines (GBMs) progressively adds distinct models to improve the precision of the predicted dependent variable. The GBM algorithm builds distinct base learners, for instance, decision trees, to

Table 4
Optimal hyperparameters values.

Algorithm	Hyperparameter	Value
RF	Number of variables “mtry”	3
	Number of trees “ntree”	60
GBM	Number of trees “n.tree”	60
	Learning rate “shrinkage”	0.2
SVM	Interaction depth “interaction.depth”	4
	Cost of constraint “C”	3
	Insensitive loss function (σ)	0.1

maximally correlate with the negative gradient of the loss function, which is linked to the full ensemble (consisting of huge moderately weak models). GBMs are comparatively simple in terms of implementation and have recorded significant breakthroughs in diverse applications [58]. Three parameters of GBMs are critical for optimal performance during tuning. The first is known as “*n.tree*”, which denotes the number of trees in the sequence. A sufficiently high number of trees is required to accomplish decent learning; however, overfitting on noisy data sets occurs when too many trees are used. Hence, monitoring “*n.tree*” is indispensable. The second parameter, the size of trees, is controlled by “*interaction.depth*” which determines the order of predictor–predictor interaction. The last parameter, *learning.rate* shrinks the contribution of each newly added tree. The smaller the (*learning.rate*) parameter, the lower the shrunk boosted increments are, thus the better the model’s generalization ability. However, this is at the cost of the convergence speed, and using a higher value for this parameter will increase the number of iterations. Three parameters were tuned using the random search method, with the optimal values depicted in Table 4.

3.4.3. Support vector machines

SVMs are used to transform high-dimensional feature data through nonlinear transformations of independent variables. SVMs tuning is essential to guarantee the sensitivity of hyperparameters throughout the vast search space. We adopt the Gaussian kernel, the default and prevalent Radial Basis Function (RBF) kernel as recommended in Meyer et al. [90]. We then optimize the regularization parameter *C*, and bandwidth σ , controlling the degree of nonlinearity, using the cross-validation technique. Table 4 portrays the optimal values of these parameters.

3.5. Performance evaluation of ML models

Models fitted to the training set were used to determine the water for a concrete mix from the training set data, whereas the test set was used for making predictions and evaluating performance measures. The same explanatory variables were used in all models. The most common practice for model validation is to evaluate the prediction ability using selected error metrics based on the test data (not used in training the model). The performance of the models was evaluated and validated using the Mean Absolute Error (MAE), Root Mean Squared Error (RMSE), Forecast Bias (B), and coefficient of determination (R^2) metrics. MAE measures the errors between paired observations, RMSE measures the spread of prediction errors (residuals) and forecast bias (B) indicates how high or low is a forecast to the actual value. The performance metrics are computed using Eqs. (6)–(9) respectively as:

- Mean Absolute Error (MAE)

$$MAE = \frac{1}{n} \sum_{i=1}^n |y_i - t_i| \quad (6)$$

- Root Mean Squared Error (RMSE)

$$RMSE = \sqrt{\frac{1}{n} \sum_{i=1}^n (y_i - t_i)^2} \quad (7)$$

- Forecast Bias (B)

$$B = \left(\frac{\sum_{i=1}^n (\bar{y} - t_i)}{n} \right)^2 \quad (8)$$

- The coefficient of determination (R^2)

$$R^2 = 1 - \frac{\sum_{i=1}^n (y_i - t_i)^2}{\sum_{i=1}^n (t_i - \bar{t}_i)^2} \quad (1)$$

where n is the number of specimens, t_i denotes observed outcomes, y_i denotes predicted outcomes, \bar{t}_i is the sample mean (i.e., $\bar{t}_i = \sum_{i=1}^n t_i/n$). The values for RMSE, MAE, forecast bias (B), and R^2 are computed for the quantity of water required by randomly sampling test data examples on fitted models (i.e., GBM, DNN, RF, SVM) and repeating this process 200 times. The sample means for these computations are then determined appropriately. Nevertheless, the applicability of the framework in this study is limited to the following cases:

- 1) Appropriate concrete mix design specifications, including required strength and slump, component content and ratio, and information about the material are used
- 2) The physical and chemical properties of cement and density are satisfactory according to general specifications.
- 3) Coarse and fine aggregates are graded within limits of generally accepted specifications.

4. Results

4.1. Performance evaluation

Table 5 and Fig. 4 summarize and compare the statistical performance metrics (MAE, RMSE, forecast bias, and R^2) of models used in this study side-by-side concerning the prediction of the required water for the concrete mix using scatter and box plots. In Table 5, the Squared-R (R^2) for fitted DNN, GBM, RF and SVM models on the test data indicated a consistent performance by DNN (0.983) compared with GBM (0.958), RF (0.954), and SVM (0.943), respectively, due to the minimal variations of the Squared-R obtained. Similarly, MAE for DNN (1.680) was better than GBM (2.078), RF (2.372) and SVM (2.343), respectively.

Also, DNN obtained the least RMSE of (2.114) compared with GBM (3.245), RF (3.459) and SVM (3.854), respectively. Concerning the difference between forecast and observed values, DNN obtained a minimum of 0.033 compared to 0.791 (GBM), 0.648 (RF), and 0.139 (SVM). Consequently, the resulting “forecast bias” measures of DNN showed a consistency in the difference between the observed outcomes and forecasts, which contrasts with other algorithms that exhibit medium or large fluctuations in error (deviation of observed and predicted values). These deviations are minimal in DNN, hence its ability to produce more reliable results.

Similarly, Fig. 5 depicts the prediction ability of the models (DNN, GBM, RF, and SVM) on the sample from the testing data to forecast the required amount of water (liter/m³) for different concrete mixes. Again, the four models predicted the amount of water required for concrete mixes with reasonable accuracy, and we perceived that the differences between the observed outcomes and forecasts are marginal for all models. However, a general outlier analysis of the plot shows that DNN has fewer outlier points than other models.

All models achieved an R^2 value (>0.94) for the correlation of the required water for concrete mixes to predictive variables. Fig. 6 depicts that the predictions by DNN, the best performing model, are accurate and closer to the measured values. This high R^2 value indicates that the

Table 5

Statistical parameters describing errors in prediction of the required water.

Models	MAE	RMSE	R^2	Bias
DNN	1.680 ± 0.11	2.114 ± 0.16	0.983 ± 0.00	0.033 ± 0.04
GBM	2.078 ± 0.23	3.245 ± 0.61	0.958 ± 0.01	0.791 ± 0.48
RF	2.392 ± 0.21	3.459 ± 0.35	0.954 ± 0.01	0.648 ± 0.47
SVM	2.343 ± 0.26	3.854 ± 0.50	0.943 ± 0.01	0.139 ± 0.18

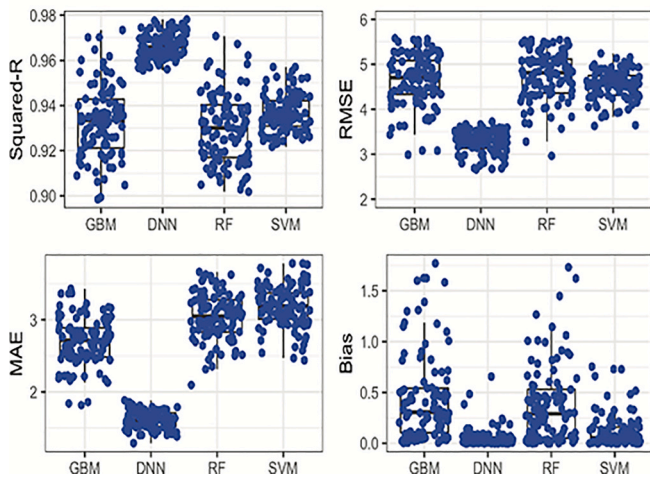


Fig. 4. Prediction plots.

required water for concrete mixes is governed by the slump, density, compressive strength, and cement, as revealed by a linear projection method with explorative data analysis depicted in Fig. 7. This linear projection method scores the attributes by computing the MSE of the k-

nearest neighbors model on a projected two-dimensional data (testing set in this case) and returning the top-scoring features that visually discriminate between different water mixes exhibited in the dataset. The top four features were presented in Fig. 7 to ensure simplicity and clarity of information.

Irrevocably, it should be noted that the comparative differences in the performance of the models are only marginal; this is possibly due to a small number of predictors used. However, the DNN model obtained the most significant improvement in prediction accuracy. These results indicate the ability of DNN to reduce unexplained variance without overfitting the data. Furthermore, the regularization techniques implemented in the DNN model avoid data overfitting, thereby providing more accurate predictions. Thus, the results of this study can be explained as follows.

- a) In comparison to other algorithms, we found that the applicability of DNN for accurate prediction of the required water in Portland concrete designs is more reliable than GBM, RF, and SVM models. The high R^2 (Figs. 4 and 6, and Table 5) values by DNN compared to other conventional machine learning methods indicate its superior prediction capability. Furthermore, the DNN explained 98% of the variability in the water content of Portland cement mixes ($R^2 = 0.983$). Thus, DNN demonstrates reasonably high predictability in managing water in the concrete mixture for adequate workability

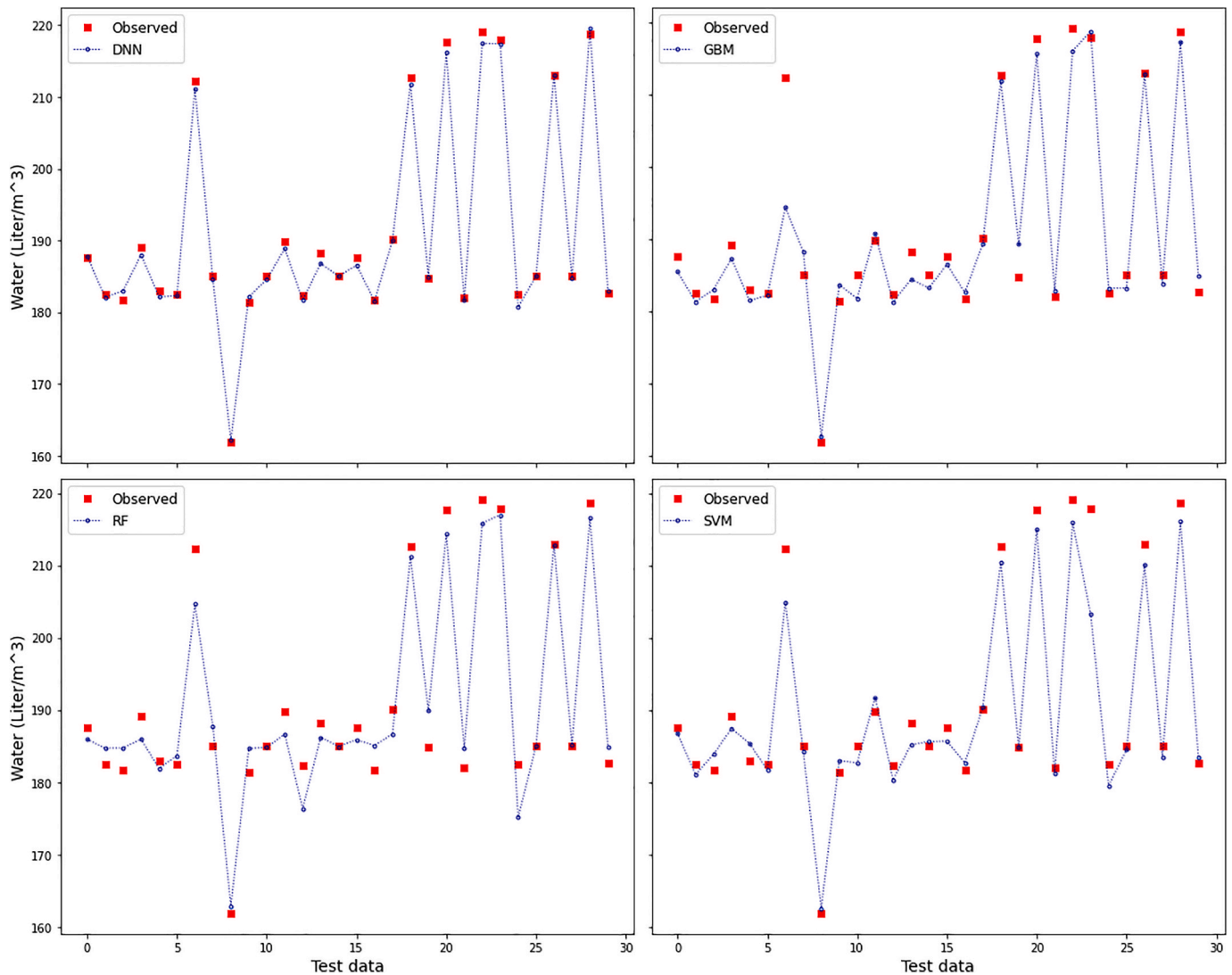


Fig. 5. Actual vs. predicted values of water (liter/m³) by models.

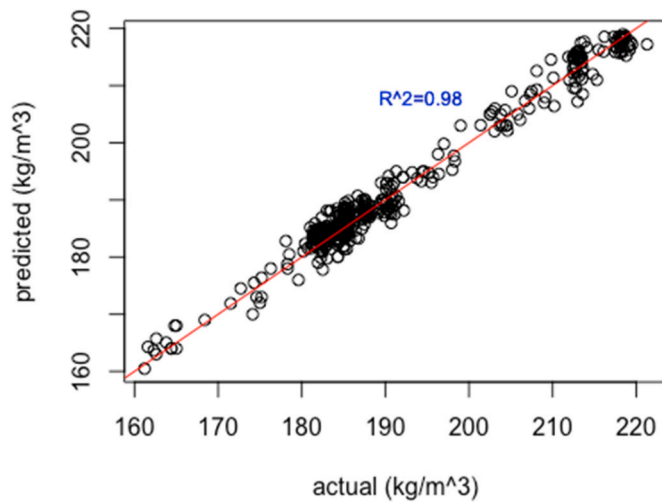


Fig. 6. Regression of test data by DNN.

and hydration optimization. The sensitivity analysis also revealed that 5-fold Cross-Validation (CV) produced a similar predictive power (i.e., $CV R^2 = 0.980$) for the required water for cement mix, confirming further that overfitting was insubstantial. The results show that the DNN model tends to accurately forecast the required water for concrete mixes.

- b) In addition, the forecast bias of DNN against other algorithms in predicting the required water for concrete mixes revealed that DNN exhibits higher accuracy, with its predictions closer to observed outcomes compared to other ML techniques, thus making it more suitable for predicting the required water for concrete mixes. Hence, the conventional methods cannot match the DNN's performance according to the evaluation criteria.

- c) Similarly, the results conformed with previous findings concerning the deep learning higher precision, higher efficiency and higher generalization ability compared with conventional ML techniques to forecast mechanical properties of concrete. For instance, deep learning techniques have been reported to exhibit higher accuracy and stronger generalization than traditional neural networks and SVM [20]; Latif [72].

4.2. DNN model interpretation

The deep neural networks are considered “black boxes” since their models are challenging and complex. Nevertheless, the interpretability of machine learning models is essential to gain insights into their behavior and facilitate the trustworthiness of their predictions. Although the main focus of this study is on the predictive performance of DNN models, it is of interest to interpret the structure of the predictive model to support model selection, criticism and development. Next, we discuss a few model-agnostic methods (i.e., measuring interactions, partial dependence, and surrogate trees) used to interpret the structure of DNN as applied to the prediction of the water quantity for concrete mix design.

Measuring interactions involves determining how strongly the features interact with each other. This interaction is measured using the H-statistic proposed by Ref. [91]. The interaction strength is zero (0) when there is no interaction and one (1) if all variations of the predicted outcome depend on a given interaction. Interactions between predictors of the DNN model are depicted in Fig. 8 (left). The predictor slump “SLMP” exhibits the strongest interaction signal, with the DNN model having the most potent interaction effect of 0.23. Other relevant predictors are density (DEN), compressive strength (CS), cement (CEM), and curing age (AG). However, coarse aggregates (CA) and fine aggregates (FA) are the least important variables in the DNN model, but both variables always contributed to the model's predictive ability. Including variables with little predictive power does not negatively affect the DNN

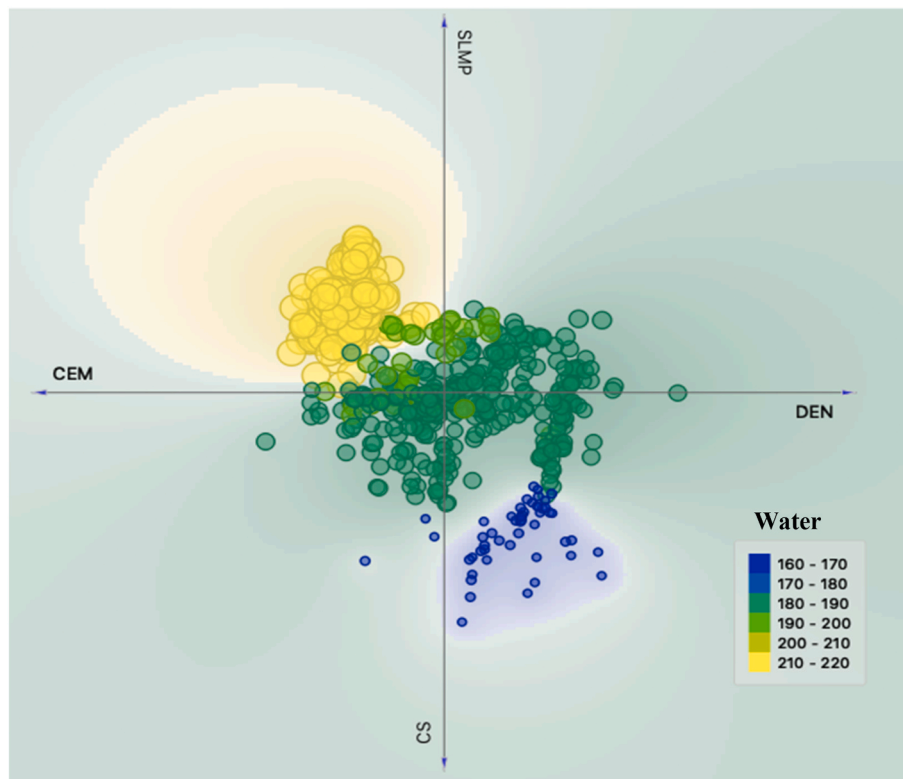


Fig. 7. Instances selected from the linear projection method.

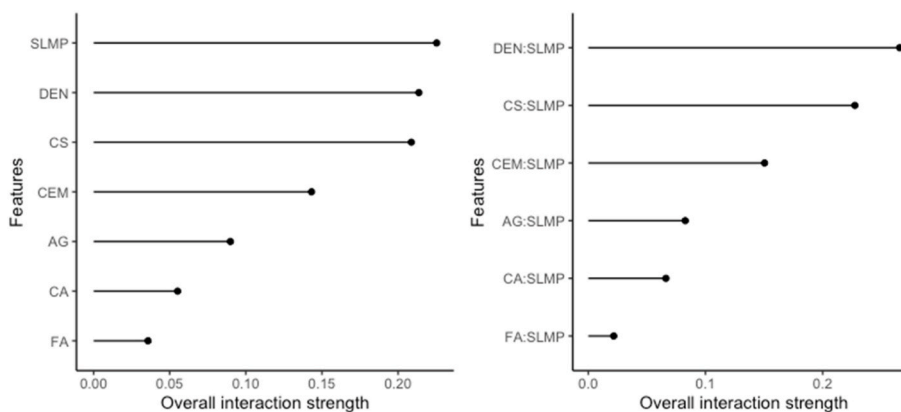


Fig. 8. Measuring interactions (left-overall interaction strength), (right- 2-way interaction).

model’s performance; therefore, there was no attempt to remove such variables from the model. Fig. 8 (right) depicts a 2-way interaction strength between slump (SLMP) and other variables. The DNN model shows density (DEN) with the strongest interaction of 0.27. Identifying these interactions is helpful in understanding which variables create co-dependencies in the model’s behavior.

Partial dependence plots (PDPs) are low dimensional graphical renderings of prediction functions to describe relationships between the outcome and predictors of interest. Partial dependence plots allow the evaluation of models and confirm how the explanatory variables are used for prediction. For example, Fig. 9 depicts ICE curves and the PDP curve (thick yellow line, averaging predictions across all observations) for comparing the marginal impact of the three key predictors (density, slump, and compressive strength) on the response variable (the required water for concrete mix). The DNN model should confirm some physical and chemical processes for the application presented here. For example, density is inversely proportional to water content, i.e., it decreases as the water content increases (Fig. 9. -left). This is attributable to the reduction of total water content leading to the lower formation of air voids in the concrete, with higher water content resulting in more air voids.

Similarly, as expected, the water content in concrete will be directly related to the slump because wetness largely determines the workability concretes. It is evident (Fig. 9. – center) that the slump increases approximately linearly with water content. Hence, the wetter the concrete, the higher the slump. Concretes with high water content have a high slump, while those with a low water content have a low slump.

Furthermore, water content (water-cement ratio) is a convenient measurement whose value is well correlated with concrete strength and durability. The lower the water content is, the higher the compressive

strength and the more durable the concrete. Fig. 10. (right) shows that the strength increases with the addition of water to facilitate the proper hydration of cement paste. However, subsequently adding more water leads to a reduction in strength, as expected. The average water required for different concrete mixes in the dataset is 186.53 L/m³, corresponding to an average w/c ratio of 0.52. This value is reasonable for the normal concrete mix as the water-cement ratio for such concrete is of moderate workability [6]. As shown in Fig. 11, the DNN model’s partial dependence plots confirmed these general predictions and processes.

Similarly, a surrogate model to interpret the internal workings of the DNN model is depicted in Fig. 10, which illustrates the use of decision trees to mimic the DNN model in respect to controlling the required water for concrete mix. These decision rules can help engineers optically control the required water in concrete mix design to facilitate the production of durable and high-quality concretes. Consequently, producing robust concretes will prevent segregation or bleeding of concrete, leading to low strength concrete that causes buildings to collapse.

5. Discussion and implication for practice

The more informed we are about concrete compositions and properties relationship, the more effective the optimization process for the concrete mix. In practice, substantial experiments are required to ensure concrete mix design meets requirements. Thus, continuous adjustment of concrete mix designs requires experience coupled with its associated complicated issues. Concrete mix modeling is to develop a system that properly reflects the very nature of the concrete mix. However, the traditional modeling techniques have shown difficulty, laborious and unreliability in predicting concrete behavior. Whereas, as evidenced by

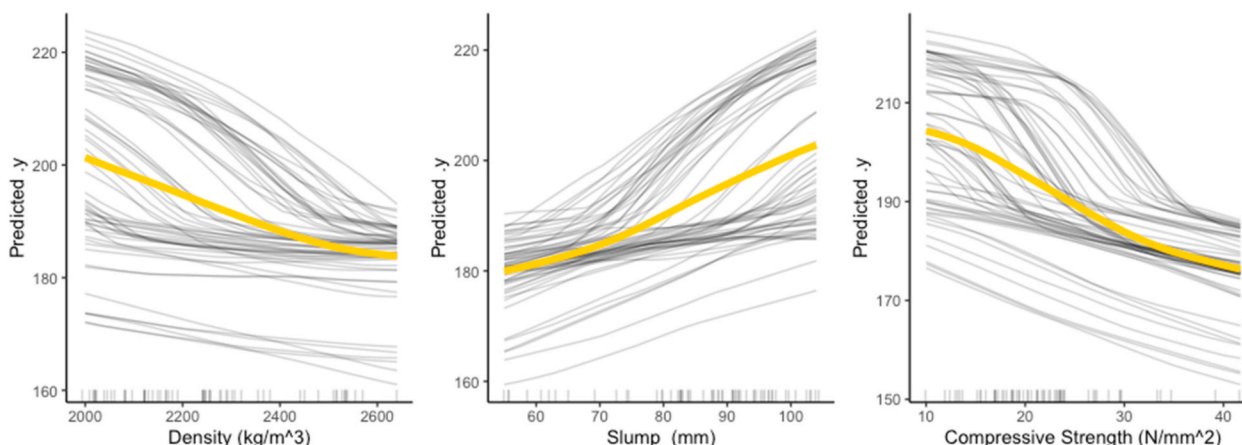


Fig. 9. Partial dependency plots for predictors “Density”, “Slump” and “Compressive strength”.

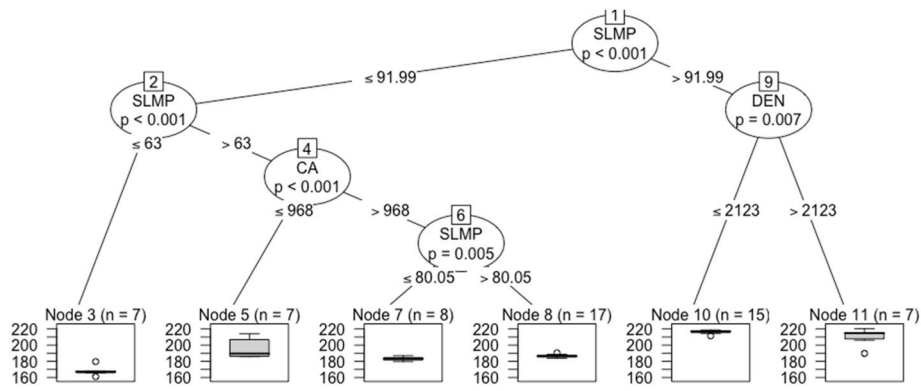


Fig. 10. DNN model interpretation with a decision tree.

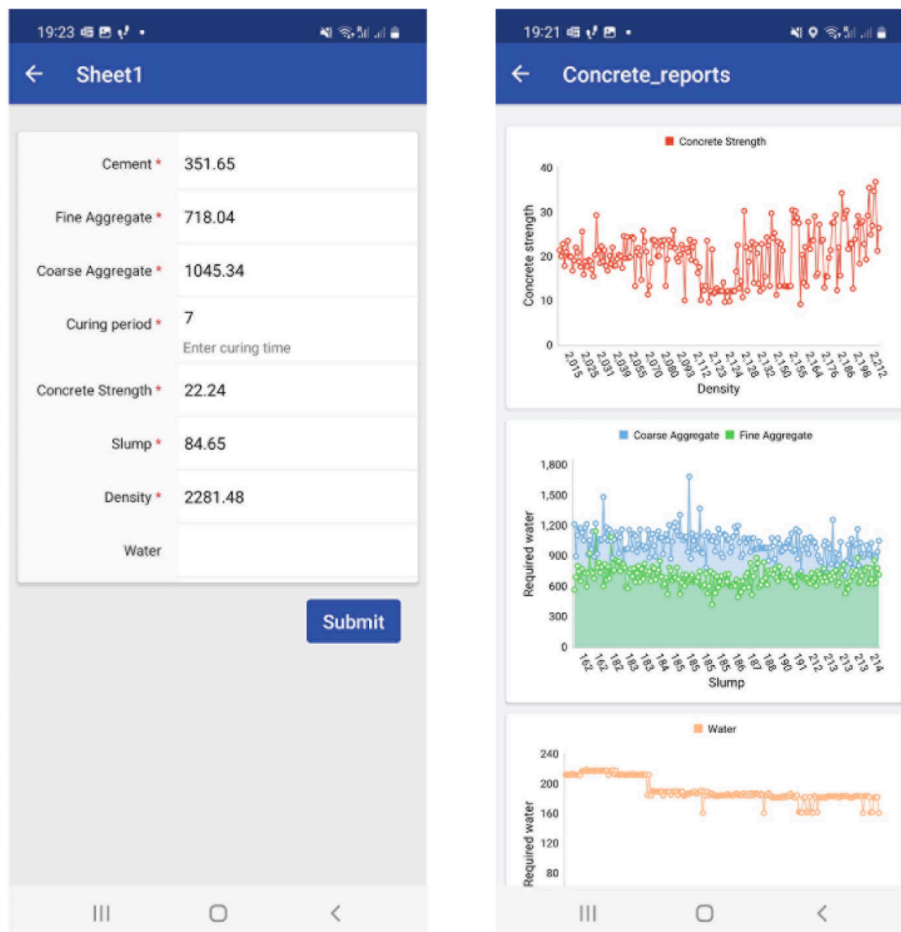


Fig. 11. A prototype tool for concrete water quantity modeling.

this study, deep learning techniques have shown considerable reliability and applicability in predicting concrete behavior. Specifically, DNN learned the complex interrelations among concrete parameters for higher accurate results and faster real-time prediction without the need for an empirical method.

In addition, to demonstrate the practical usefulness of this model, its prototype was developed to enable civil engineers and other users to make practical, informed decisions in the field regarding managing the complexity of the concrete material behavior to control the concrete water content. Users supply appropriate input parameters through the user interface, which triggers the DNN model to predict the required water content and presents justifications for arriving at any decision.

Similarly, the tool allows for effective collection and storage of new data to address the data limitation problem. Fig. 9 depicts sample screenshots of the tool, which enable civil engineers to model the required water for concrete mixes without performing a series of trial mixes.

The assumption made in this study is that the nature of constituent materials (types and shapes of aggregates, cement brands, mixing techniques, and other components) is constant and that only water content is a varying factor. By this assumption, the effect of water is considered to have an overbearing impact on the concrete strength, and the effects of other factors could be considered secondary.

Developing this tool has tremendous application in the field of concrete technology or practice, specifically, the calibration of mixing

power of the concrete water content for improved water control accuracy. By the results of this study, the dilemma of what quantity of water is required to achieve optimum strength would be reduced if not eliminated. The tool will also allow concrete practitioners to simulate concrete strength containing different constituents before starting the trials mix, thus reducing the number of trials needed to achieve the desired strength. Also, the tool will be helpful for educational purposes by demonstrating how constituent materials vary with compressive strengths at varied water-cement ratios.

While the previous studies developed predictive models for specialized concrete types such as HPC blended concrete, other authors measured other mechanical properties. However, the current study developed a predictive model for the required quantity of water at different compressive strengths for the standard regular concrete. Since improvement on the compressive strength of concrete will lead to improvement of the durability of concrete. This study considered regular concrete, where chemical and(or) mineral admixtures in concrete production are optional. For example, where high compressive strength may not be of high interest (i.e., construction of dams), the durability of the concrete may be paramount. In that case, supplementary cementitious materials, i.e., fly ash and ground granulated blast slag (GGBS), may be included in the concrete to reduce the high heat of hydration of normal cement, which often leads to internal cracks. This specialized concrete may be on a special request as fly ash and GGBS are not readily available, particularly in most parts of Africa.

Consequently, the contribution of this study is to develop a robust model to estimate the required water content (water to cement ratio) in concrete mixtures as maintaining the quality of hardened products for short or long terms is demanding. Therefore, a theoretical implication of the study is the implementation of a deep learning model suitable for predicting the required water of concrete mix based on the constituent materials after 7, 14, and 28-days of curing. In addition, the developed deep learning model showed superior accuracy to other conventional machine learning techniques and had the most improved statistical parameter values (RMSE = 2.114, MAE = 1.680, $R^2 = 0.983$) for the test data. Furthermore, in practical terms, the developed model will facilitate efficient control of water contents in concrete with no chemical admixtures and prevent frequent building collapse due to poor-quality concrete, where superplasticizer is unpopular because of additional costs. Also, in addressing the “black box” challenge associated with current ML models, we adopt relevant model-agnostic approaches to gain insights into the proposed deep learning model for concrete water content prediction to facilitate the trustworthiness and transparency of its predictions.

Also, further refinement in the ML approach, as shown by the deep learning model, has helped substantially reduce material wastage and production time and improve concrete quality. Furthermore, the developed model is easily accessible to onsite construction workers for consultation. Thus, the discovered knowledge will assist experts to optimize concrete mix design for improved production at a lower cost, which will eventually reflect in the concrete maintenance and life cycle cost.

6. Conclusion

This study is vital in determining the required quantity of water for improved water control accuracy of concrete mix to guarantee high-quality concretes without chemical admixture using state-of-the-art deep neural networks. Furthermore, the proposed tool improves the accuracy of concrete water prediction and modeling in concrete mixes to reduce and eliminate wastes due to collapsed concrete structures resulting from incorrect concrete mixes. The statistical analysis of the DNN model in predicting the required water for the concrete mix was done by evaluating and validating its prediction ability with conventional machine learning methods using RMSE, MAE, forecast bias, and R^2 as performance metrics. The values of RMSE, MAE, forecast bias, and

R^2 obtained were 2.114, 1.680, 0.033, and 0.983, respectively, on the testing set. Thus, the formulated computational model for predicting the required water for the concrete mix showed good results, as the differences between the forecasts and observed outcomes are negligible. Furthermore, in comparison with other conventional machine learning models, DNN gave the most negligible forecast bias, RMSE, and MAE values, and the highest R-Squared (0.983). This result revealed a high correlation between the experimental results and forecasts from DNN, thus, proving its suitability in predicting the required water for the concrete mix.

The outcome of this study can aid civil engineers and related professionals in the precise determination of the required water for different concrete mixes without performing a series of laboratory tests or trials mix, thereby leading to reduced construction wastes and consequently reduced environmental impacts. In addition, the results of this study can be used to formulate industry guidelines to predict the water-cement ratio in ready-mix concrete production. The novelty of applying the proposed model is its simplicity and ease of application. Many of the existing models are complex to use while on site. This study can also influence further academic research in the use of multilayer feedforward networks to formulate water-cement ratios for different concrete mixes and related studies.

It should be noted that fewer predictors of concrete water are used in this study; in the future, we hope to incorporate more predictors, such as density and sizes of the coarse and fine aggregates, workability and setting time of cement and concrete. In addition, the inclusion of more data records, i.e., ambient temperature, pressure, and humidity in the dataset, will further improve prediction performance. Also, we hope to incorporate image processing techniques to enhance the prediction process. We also hope to get concrete mix design data from more sources to improve the robustness of the model. Furthermore, we will carry out an analysis of different DNN architectures for better insight.

CRedit author statement

Sururah Bello: Conceptualization, Supervision, Resources, Writing – review & editing. **Lukumon Oyedele:** Visualization, Resources, Writing – review & editing. **Olakunle Kazeem Olaitan:** Investigation, Methodology, Formal analysis, Writing – original draft, Preparation. **Kolawole Olonade:** Supervision, Data curation, Resources, Writing – review & editing. **Akinropo Musiliu Olajumoke:** Supervision, Writing – review & editing. **Anuoluwapo Ajayi:** Formal analysis, Writing – review & editing. **Lukman Akanbi:** Writing – review & editing. **Olugbenga Akinade:** Writing – review & editing. **Mistura Sanni:** Formal analysis. **Abdul-Lateef Bello:** Data Curation and Writing.

Declaration of competing interest

The authors declare that they have no known competing financial interests or personal relationships that could have appeared to influence the work reported in this paper.

Acknowledgement

The authors would like to express their appreciation to the Engineering and Physical Science Research Council (EPSRC) United Kingdom (Grant Ref: EP/S031480/1) for providing the financial support for this study.

References

- [1] V. Živica, Effects of the very low water/cement ratio, *Construct. Build. Mater.* 23 (2009) 3579–3582.
- [2] J. Liu, Quality prediction for concrete manufacturing, *Autom. Construct.* 5 (1997) 491–499.

- [3] I.E. Umeonyiagu, C.C. Nwobi-Okoye, Modelling compressive strength of concretes incorporating termite mound soil using multi-layer perceptron networks: a case study of eastern Nigeria, *Int. J. Res. Rev. Appl. Sci.* 24 (2015) 19.
- [4] R.O. Oduola, Poor quality concrete: a major challenge in the building construction industry in Nigeria, in: *Struct. Archit. - Proc. 1st Int. Conf. Struct. Archit. ICSA 2010*, 2010, pp. 1642–1650.
- [5] A.M. Olajumoke, I.A. Oke, A.B. Fajobi, M.O. Ogedengbe, Engineering failure analysis of a failed building in Osun State, Nigeria, *J. Fail. Anal. Prev.* 9 (2009) 8–15, <https://doi.org/10.1007/s11668-008-9197-7>.
- [6] A.M. Neville, *Properties of Concrete*, Fourth, Pitman, London, 2011.
- [7] N. Liu, Quality prediction for concrete manufacturing, *Autom. Construct.* 5 (6) (1997) 491–499.
- [8] X.X. Zhang, X. Qiao, X. Wu, The relationship of water-cement ratio to the strength of cemented tailing-waste rocks, *Adv. Mater. Res.* 1030–1032 (2014) 926–931.
- [9] S. Popovics, J. Ujhelyi, Contribution to the concrete strength versus water cement ratio relationship, *J. Mater. Civ. Eng.* 20 (2008) 459–463.
- [10] A.M. Olajumoke, I.A. Oke, K.A. Olonade, A.A. Laoye, Effects of non-potable water on the strengths of concrete, *Ife J. Technol. Fac. Technol. Obafemi Awolowo Univ. Ile-Ife*. 21 (2012) 38–42.
- [11] T. Nagaraj, Z. Banu, Generalization of Abrams' law, *Cement Concr. Res.* 26 (1996) 933–942.
- [12] K.C. Hover, The influence of water on the performance of concrete, *Construct. Build. Mater.* 25 (2011) 3003–3013, <https://doi.org/10.1016/j.conbuildmat.2011.01.010>.
- [13] G. Andreu, E. Miren, Experimental analysis of properties of high performance recycled aggregate concrete, *Construct. Build. Mater.* 52 (2014) 227–235, <https://doi.org/10.1016/j.conbuildmat.2013.11.054>.
- [14] R.V. Silva, J. De Brito, R.K. Dhir, The influence of the use of recycled aggregates on the compressive strength of concrete: a review, *Eur. J. Environ. Civ. Eng.* 19 (2015) 825–849, <https://doi.org/10.1080/19648189.2014.974831>.
- [15] W. Chen, P. Shen, Z. Shui, Determination of water content in fresh concrete mix based on relative dielectric constant measurement, *Construct. Build. Mater.* 34 (2012) 306–312, <https://doi.org/10.1016/j.conbuildmat.2012.02.073>.
- [16] M. Açikgenç, M. Ulaş, K.E. Alyamaç, Using an artificial neural network to predict mix compositions of steel fiber-reinforced concrete, *Arabian J. Sci. Eng.* 40 (2015) 407–419, <https://doi.org/10.1007/s13369-014-1549-x>.
- [17] W. Schmidt, I.L.T. Ngassam, K.A. Olonade, R. Mbugua, H. Kühne, Plant based chemical admixtures – potentials and effects on the performance of cementitious materials, *RILEM Tech. Lett.* 3 (2018) 124–128.
- [18] S. Popovics, Analysis of concrete strength versus water-cement ratio relationship, *Mater. J.* 87 (5) (1990) 517–529.
- [19] M.F.M. Zain, S.M. Abd, Multiple regression model for comprehensive strength prediction of high performance concrete, *J. Appl. Sci.* 9 (2009) 155–160.
- [20] F. Deng, Y. He, S. Zhou, Y. Yu, H. Cheng, X. Wu, Compressive strength prediction of recycled concrete based on deep learning, *Construct. Build. Mater.* 175 (2018) 562–569, <https://doi.org/10.1016/j.conbuildmat.2018.04.169>.
- [21] J.R. Jang, ANFIS: adaptive-network-based fuzzy inference system, *IEEE Trans. Syst. Man Cyber.* 23 (1993) 665–685.
- [22] I.C. Yeh, Modeling of strength of high-performance concrete using artificial neural networks, *J. Civ. Eng.* 28 (1998) 1797–1808.
- [23] S.C. Lee, Prediction of concrete strength using artificial neural networks, *Eng. Struct.* 25 (2003) 849–857.
- [24] R. Gupta, M.A. Kewalramani, A. Goel, Prediction of concrete strength using neural-expert system, *J. Mater. Civ. Eng.* 18 (2006) 462–466.
- [25] A. Oreta, K. Kawashima, Neural network modeling of confined compressive strength and strain of circular concrete columns, *J. Struct. Eng.* 129 (2003).
- [26] R. Ince, Prediction of fracture parameters of concrete by artificial neural networks, *Eng. Fract. Mech.* 71 (2004) 2143–2159, <https://doi.org/10.1016/j.engfractmech.2003.12.004>.
- [27] Z.H. Duan, S.C. Kou, C.S. Poon, Using artificial neural networks for predicting the elastic modulus of recycled aggregate concrete, *Construct. Build. Mater.* 44 (2013) 524–532, <https://doi.org/10.1016/j.conbuildmat.2013.02.064>.
- [28] M.M. Alshihri, A.M. Azmy, M.S. El-Bisy, Neural networks for predicting compressive strength of structural light weight concrete, *Construct. Build. Mater.* 23 (2009) 2214–2219, <https://doi.org/10.1016/j.conbuildmat.2008.12.003>.
- [29] M. Pala, E. Özbay, A. Öztaş, M.I. Yuce, Appraisal of long-term effects of fly ash and silica fume on compressive strength of concrete by neural networks, *Construct. Build. Mater.* 21 (2007) 384–394, <https://doi.org/10.1016/j.conbuildmat.2005.08.009>.
- [30] M.I. Khan, Predicting properties of high performance concrete containing composite cementitious materials using artificial neural networks, *Autom. Construct.* 22 (2012) 516–524, <https://doi.org/10.1016/j.autcon.2011.11.011>.
- [31] C. Bilim, C.D. Atiş, H. Tanyildizi, O. Karahan, Predicting the compressive strength of ground granulated blast furnace slag concrete using artificial neural network, *Adv. Eng. Software* 40 (2009) 334–340, <https://doi.org/10.1016/j.advengsoft.2008.05.005>.
- [32] R. Parichatprecha, P. Nimityongskul, Analysis of durability of high performance concrete using artificial neural networks, *Construct. Build. Mater.* 23 (2009) 910–917, <https://doi.org/10.1016/j.conbuildmat.2008.04.015>.
- [33] Z.H. Duan, S.C. Kou, C.S. Poon, Prediction of compressive strength of recycled aggregate concrete using artificial neural networks, *Construct. Build. Mater.* 40 (2013) 1200–1206, <https://doi.org/10.1016/j.conbuildmat.2012.04.063>.
- [34] J. Shao, X. Ji, R. Li, Application of BP neural network model in the recycled concrete performance prediction, in: *International Conference on Advances in Energy, Environment and Chemical Engineering (AEECE)*, 2015, pp. 527–532.
- [35] G. Trtnik, F. Kavčič, G. Turk, Prediction of concrete strength using ultrasonic pulse velocity and artificial neural networks, *Ultrasonics* 49 (2009) 53–60, <https://doi.org/10.1016/j.ultras.2008.05.001>.
- [36] M. Bilgehan, P. Turgut, The use of neural networks in concrete compressive strength estimation, *Comput. Concr.* 7 (2010) 271–283, <https://doi.org/10.12989/cac.2010.7.3.271>.
- [37] M.A. Kewalramani, R. Gupta, Concrete compressive strength prediction using ultrasonic pulse velocity through artificial neural networks, *Autom. Construct.* 15 (2006) 374–379.
- [38] F. Özcan, C.D. Atiş, O. Karahan, E. Uncuoğlu, H. Tanyildizi, Comparison of artificial neural network and fuzzy logic models for prediction of long-term compressive strength of silica fume concrete, *Adv. Eng. Software* 40 (2009) 856–863, <https://doi.org/10.1016/j.advengsoft.2009.01.005>.
- [39] I.C. Yeh, Modeling slump flow of concrete using second-order regressions and artificial neural networks, *Cem. Concr. Compos.* 29 (2007) 474–480, <https://doi.org/10.1016/j.cemconcomp.2007.02.001>.
- [40] U. Atici, Prediction of the strength of mineral admixture concrete using multivariable regression analysis and an artificial neural network, *Expert Syst. Appl.* 38 (2011) 9609–9618, <https://doi.org/10.1016/j.eswa.2011.01.156>.
- [41] I.B. Topçu, M. Sarıdemir, Prediction of compressive strength of concrete containing fly ash using artificial neural networks and fuzzy logic, *Comput. Mater. Sci.* 41 (2008) 305–311.
- [42] M.H.F. Zarandi, I.B. Türksen, J. Sobhani, A.A. Ramezani-pour, Fuzzy polynomial neural networks for approximation of the compressive strength of concrete, *Appl. Soft Comput.* 8 (2008) 488–498.
- [43] N.B. Siraj, A.R. Fayek, A.A. Tsehayae, Development and optimization of artificial intelligence-based concrete compressive strength predictive models, *Int. J. Struct. Civ. Eng. Res.* 5 (2016) 156–167, <https://doi.org/10.18178/ijscer.5.3.156-167>.
- [44] I.C. Yeh, L.C. Lien, Knowledge discovery of concrete material using Genetic Operation Trees, *Expert Syst. Appl.* 36 (2009) 5807–5812, <https://doi.org/10.1016/j.eswa.2008.07.004>.
- [45] J. Sobhani, M. Najimi, A.R. Pourkhorshidi, T. Parhizkar, Prediction of the compressive strength of no-slump concrete: a comparative study of regression, neural network and ANFIS models, *Construct. Build. Mater.* 24 (2010) 709–718, <https://doi.org/10.1016/j.conbuildmat.2009.10.037>.
- [46] S.S. Gilan, H.B. Jovein, A.A. Ramezani-pour, Hybrid support vector regression - particle swarm optimization for prediction of compressive strength and RCPT of concretes containing metakaolin, *Construct. Build. Mater.* 34 (2012) 321–329, <https://doi.org/10.1016/j.conbuildmat.2012.02.038>.
- [47] M. Castelli, L. Vanneschi, S. Silva, Prediction of high performance concrete strength using Genetic Programming with geometric semantic genetic operators, *Expert Syst. Appl.* 40 (2013) 6856–6862, <https://doi.org/10.1016/j.eswa.2013.06.037>.
- [48] H.I. Erdal, Two-level and hybrid ensembles of decision trees for high performance concrete compressive strength prediction, *Eng. Appl. Artif. Intell.* 26 (2013) 1689–1697, <https://doi.org/10.1016/j.engappai.2013.03.014>.
- [49] Z. Yuan, L.N. Wang, X. Ji, Prediction of concrete compressive strength: research on hybrid models genetic based algorithms and ANFIS, *Adv. Eng. Software* 67 (2014) 156–163, <https://doi.org/10.1016/j.advengsoft.2013.09.004>.
- [50] A. Behnood, J. Olek, M.A. Glinicki, Predicting modulus elasticity of recycled aggregate concrete using M5' model tree algorithm, *Construct. Build. Mater.* 94 (2015) 137–147, <https://doi.org/10.1016/j.conbuildmat.2015.06.055>.
- [51] M.Y. Cheng, N.D. Hoang, A self-adaptive fuzzy inference model based on least squares SVM for estimating compressive strength of rubberized concrete, *Int. J. Inf. Technol. Decis. Making* 15 (2016) 603–619.
- [52] I. González-Taboada, B. González-Fontboa, F. Martínez-Abella, J.L. Pérez-Ordóñez, Prediction of the mechanical properties of structural recycled concrete using multivariable regression and genetic programming, *Construct. Build. Mater.* 106 (2016) 480–499, <https://doi.org/10.1016/j.conbuildmat.2015.12.136>.
- [53] I. Miličević, T.K. Šipos, Prediction of properties of recycled aggregate concrete, *J. Croat. Assoc. Civ. Eng.* 69 (2017) 347–357, <https://doi.org/10.14256/jce.1867.2016>.
- [54] R.A. Mozumder, B. Roy, A.I. Laskar, Support vector regression approach to predict the strength of FRP confined concrete, *Arabian J. Sci. Eng.* 42 (2017) 1129–1146, <https://doi.org/10.1007/s13369-016-2340-y>.
- [55] Z.M. Yaseen, R.C. Deo, A. Hilal, A.M. Abd, L.C. Bueno, S. Salcedo-Sanz, M.L. Nehdi, Predicting compressive strength of lightweight foamed concrete using extreme learning machine model, *Adv. Eng. Software* 115 (2018) 112–125, <https://doi.org/10.1016/j.advengsoft.2017.09.004>.
- [56] Vinay Chandwani, V. Agrawal, R. Nagar, Modeling slump of ready mix concrete using genetic algorithms assisted training of Artificial Neural Networks, *Expert Syst. Appl.* 42 (2015) 885–893, <https://doi.org/10.1016/j.eswa.2014.08.048>.
- [57] T. Han, A. Siddique, K. Khayat, J. Huang, A. Kumar, An ensemble machine learning approach for prediction and optimization of modulus of elasticity of recycled aggregate concrete, *Construct. Build. Mater.* 244 (2020), 118271, <https://doi.org/10.1016/j.conbuildmat.2020.118271>.
- [58] J. Zhang, D. Li, Y. Wang, Toward intelligent construction: prediction of mechanical properties of manufactured-sand concrete using tree-based models, *J. Clean. Prod.* 258 (2020), 120665, 2020.
- [59] C. Yeh, Design of High-performance concrete mixture using neural networks and nonlinear programming, *J. Comput. Civ. Eng.* 13 (1999) 36–42.
- [60] A. Krizhevsky, I. Sutskever, G.E. Hinton, ImageNet classification with deep convolutional neural networks, in: *Adv. Neural Inf. Processing Syst.*, 2012, pp. 1097–1105.

- [61] Y. Dong, G. Hinton, N. Morgan, Introduction to the special section on deep learning for speech and language processing, *IEEE Trans. Audio Speech Lang. Process.* 20 (2012) 4–6.
- [62] Y.J. Cha, W. Choi, O. Büyükköztürk, Deep learning-based crack damage detection using convolutional neural networks, *Comput. Civ. Infrastruct. Eng.* 32 (2017) 361–378, <https://doi.org/10.1111/mice.12263>.
- [63] L. Jing, M. Zhao, P. Li, X. Xu, A convolutional neural network based feature learning and fault diagnosis method for the condition monitoring of gearbox, *Meas. J. Int. Meas. Confed.* 111 (2017) 1–10, <https://doi.org/10.1016/j.measurement.2017.07.017>.
- [64] A. Ajayi, L. Oyedele, H. Owolabi, O. Akinade, M. Bilal, J.M. Davila Delgado, L. Akanbi, Deep learning models for health and safety risk prediction in power infrastructure, *Proj. Risk Anal. risa.* 13425 (2020), <https://doi.org/10.1111/risa.13425>.
- [65] L. Akanbi, A. Oyedele, L. Oyedele, R. Salami, Deep Learning Model for Demolition Waste Prediction in a Circular Economy, *J. Clean. Prod. Artic. Press*, 2020.
- [66] Y. Tang, R. Salakhutdinov, G. Hinton, Robust Boltzmann machines for recognition and denoising, in: *IEEE Conference on Computer Vision and Pattern Recognition (CVPR)*, IEEE, RI, USA, 2012.
- [67] A. Oyedele, A. Ajayi, L.O. Oyedele, J.M.D. Delgado, L. Akanbi, O. Akinade, H. Owolabi, M. Bilal, Deep learning and Boosted trees for injuries prediction in power infrastructure projects, *Appl. Soft Comput.* 110 (2021), 107587.
- [68] Xudong Qu, J. Yang, M. Chang, A deep learning model for concrete dam deformation prediction based on RS-LSTM, *J. Sens.* (2019) 14–4581672.
- [69] Q. Ren, M. Li, H. Li, Y. Shen, A novel deep learning prediction model for concrete dam displacements using interpretable mixed attention mechanism, *Adv. Eng. Inf.* 50 (2021), 101407.
- [70] L. Yang, X. An, S. Du, Estimating workability of concrete with different strength grades based on deep learning, *Measurement* 186 (2021), 110073.
- [71] Y. Song, Z. Huang, C. Shen, H. Shi, D.A. Lange, Deep learning-based automated image segmentation for concrete petrographic analysis, *Cement Concr. Res.* 135 (2020), 106118.
- [72] S.D. Latif, Concrete compressive strength prediction modeling utilizing deep learning long short-term memory algorithm for a sustainable environment, *Environ. Sci. Pollut. Res.* 28 (2021) 30294–30302.
- [73] H. Tanyildizi, A. Şengür, Y. Akbulut, M. Şahin, Deep learning model for estimating the mechanical properties of concrete containing silica fume exposed to high temperatures, *Front. Struct. Civ. Eng.* 14 (2020) 1316–1330.
- [74] M. Flah, A.R. Suleiman, M.L. Nehd, Classification and quantification of cracks in concrete structures using deep learning image-based techniques, *Cement Concr. Compos.* 114 (2020), 103781.
- [75] F. Wei, G. Yang, Y. Sun, Instance-level recognition and quantification for concrete surface bughole based on deep learning, *Autom. Construct.* 107 (2019), 102920.
- [76] Y. LeCun, Y. Bengio, G. Hinton, Deep learning, *Nature* 521 (2015) 436–444.
- [77] J. Schmidhuber, Deep Learning in neural networks: an overview, *Neural Network* 61 (2015) 85–117, <https://doi.org/10.1016/j.neunet.2014.09.003>.
- [78] R. Miikkulainen, J. Liang, E. Meyerson, A. Rawal, D. Fink, O. Francon, B. Raju, H. Shahrzad, A. Navruzyan, N. Duffy, B. Hodjat, Chapter 15 - evolving deep neural networks, in: Robert Kozma, Cesare Alippi, F.C.M. Yoonsuck Choe (Eds.), *Artificial Intelligence in the Age of Neural Networks and Brain Computing*, Academic Press, 2019, pp. 293–312.
- [79] X. Glorot, A. Bordes, Y. Bengio, Deep sparse rectifier networks, *AISTATS* 15 (2011) 315–323.
- [80] M. Ranzato, Y.L. Boureau, Y. Le Cun, Sparse feature learning for deep belief networks, in: *Adv. Neural Inf. Process. Syst. 20 - Proc. 2007 Conf.*, 2009, pp. 1–8.
- [81] A. Candel, V. Parmar, E. LeDell, A. Arora, Deep Learning with H2O, Mt. View, 2015.
- [82] P.K. Mehta, P.J.M. Monteiro, *Concrete: Microstructure, Properties, and Materials*, McGraw Hill, 2006, p. 659.
- [83] M.S. Shetty. *Concrete technology, theory and practice*, S. Chand and Co Ltd, England, 2006.
- [84] A.N. Ede, O.M. Olofinnade, G.O. Bamigboye, K.K. Shittu, E.I. Ugwu, Prediction of fresh and hardened properties of normal concrete via choice of aggregate sizes, concrete mix-ratios and cement, *Int. J. Civ. Eng. Construct. Technol.* 8 (10) (2017) 288–301.
- [85] G. James, D. Witten, T. Hastie, R. Tibshirani, *An introduction to statistical learning: with applications in R*, in: 2013, Corr. 7th Printing 2017 Edition, first ed., Springer, 2013.
- [86] X. Chu, I.F. Ilyas, S. Krishnan, J. Wang, Data cleaning: Overview and emerging challenges, in: *In Proceedings of the 2016 international conference on management of data*, 2016, pp. 2201–2206.
- [87] Y. Nesterov, A method for unconstrained convex minimization problem with the rate of convergence $O(1/k^2)$, *Am. Math. Soc.* 27 (1983), 372–276.
- [88] L. Breiman, Statistical modeling: the two cultures (with comments and a rejoinder by the author, *Stat. Sci.* 16 (3) (2001) 199–231.
- [89] J.H. Friedman, Greedy function approximation: a gradient boosting machine, *Ann. Stat.* (2001) 1189–1232.
- [90] <https://arxiv.org/abs/1705.09780>, 2017. (Accessed 12 January 2022).
- [91] J. Friedman, B. Popescu, Predictive learning via rule ensembles, *Ann. Appl. Stat.* 2 (2008) 916–954.